

# On the efficiency of production of the Fe K $\alpha$ emission line in neutral matter

T. Yaqoob<sup>1</sup>, K. D. Murphy<sup>2</sup>, L. Miller<sup>3</sup> and T. J. Turner<sup>4</sup>

<sup>1</sup>*Department of Physics and Astronomy, Johns Hopkins University, Baltimore, MD 21218.*

<sup>2</sup>*MIT Kavli Institute for Astrophysics and Space Research, 77 Massachusetts Avenue, NE80-6013, Cambridge, MA 02139.*

<sup>3</sup>*Department of Physics, University of Oxford, Denys Wilkinson Building, Keble Road, Oxford, OX1 3RH, UK.*

<sup>4</sup>*Department of Physics, University of Maryland Baltimore County, 1000 Hilltop Circle, Baltimore, MD 21250, USA.*

Accepted. Received; in original form

## ABSTRACT

The absolute luminosity of the Fe K $\alpha$  emission line from matter illuminated by X-rays in astrophysical sources is nontrivial to calculate except when the line-emitting medium is optically-thin to absorption and scattering. We characterize the Fe K $\alpha$  line flux using a dimensionless efficiency, defined as the fraction of continuum photons above the Fe K shell absorption edge threshold energy that appear in the line. The optically-thin approximation begins to break down even for column densities as small as  $2 \times 10^{22} \text{ cm}^{-2}$ . We show how to obtain reliable estimates of the Fe K $\alpha$  line efficiency in the case of cold, neutral matter, even for the Compton-thick regime. We find that, regardless of geometry and covering factor, the largest Fe K $\alpha$  line efficiency is attained well before the medium becomes Compton-thick. For cosmic elemental abundances it is difficult to achieve an efficiency higher than a few percent under the most favorable conditions and lines of sight. For a given geometry, Compton-thick lines-of-sight may have Fe K $\alpha$  line efficiencies that are orders of magnitude less than the maximum possible for that geometry. Configurations that allow unobscured views of a Compton-thick reflecting surface are capable of yielding the highest efficiencies. Our results can be used to estimate the predicted flux of the narrow Fe K $\alpha$  line at  $\sim 6.4$  keV from absorption models in AGN. In particular we show that contrary to a recent claim in the literature, absorption-dominated models for the relativistic Fe K $\alpha$  emission line in MCG –6-30-15 *do not* over-predict the narrow Fe K $\alpha$  line for any column density or covering factor.

**Key words:** galaxies: active - galaxies:individual: MCG –6-30-15 - line:formation - radiation mechanism: general - scattering - X-rays: general

## 1 INTRODUCTION

The narrow (FWHM  $< 10^4 \text{ km s}^{-1}$ ) fluorescent Fe K $\alpha$  emission line at  $\sim 6.4$  keV is a ubiquitous feature in the X-ray spectra of both type 1 and type 2 active galactic nuclei (AGNs), its centroid energy indicating an origin in cold, neutral matter (e.g. Sulentic et al. 1998; Yaqoob & Padmanabhan 2004; Levenson et al. 2006, and references therein). The Fe K $\alpha$  line at  $\sim 6.4$  keV is also an important diagnostic in some X-ray binary systems (e.g. White et al. 1995; Watanabe et al. 2003; Paul et al. 2005; Miller 2007, and references therein). The equivalent width (EW) and luminosity of the Fe K $\alpha$  line are nontrivial to calculate, except when the total Fe K band ( $\sim 6\text{--}7$  keV) optical depth of the line to absorption and scattering is  $\ll 1$ . In general, the observed EW and line flux depend, at the very least, on the geometry, column

density of the line-emitting matter, covering factor, element abundances, and the orientation of the structure relative to the observer’s line of sight. Using cosmic abundances from Anders & Grevesse (1989) and photoelectric cross-section from Verner et al. (1996), it is straightforward to show that the optical depth of the Fe K $\alpha$  line to absorption plus Compton scattering is  $\tau_{\text{tot}} \sim 0.027 N_{22}$ , where  $N_{22}$  is the column density,  $N_H$ , in units of  $10^{22} \text{ cm}^{-2}$ . Thus,  $\tau_{\text{tot}}$  is already  $\sim 0.1$  for column densities as low as  $4 \times 10^{22} \text{ cm}^{-2}$  so that we expect EWs and line fluxes calculated using an optically-thin approximation to break down even for column densities lower than  $\sim 10^{23} \text{ cm}^{-2}$ . Indeed, using detailed Monte Carlo simulations of a toroidal X-ray reprocessor, Murphy & Yaqoob (2009; hereafter MY09) showed that geometrical and inclination-angle effects begin to become important for  $N_H \sim 10^{23} \text{ cm}^{-2}$ .

Whilst detailed calculations of the Fe K $\alpha$  line EW for various geometries are abundant in the literature (e.g. Leahy & Creighton 1993; Ghisellini et al. 1994; Krolik et al. 1994; Nandra & George 1994; Matt et al. 1999; Ikeda, Awaki, & Terashima 2009; MY09), detailed information on the Fe K $\alpha$  line *flux* (or luminosity) is lacking. In some situations, one may be interested in the absolute flux of the Fe K $\alpha$  line (in addition to, or instead of the EW). For example, we may want to know the fraction of the number of photons (or fraction of the luminosity) in the continuum above the Fe K photoelectric absorption edge threshold energy that appear in the Fe K $\alpha$  emission line. Since the reprocessed, scattered X-ray continuum at any particular energy is a complicated function of the column density, geometry, and system inclination angle, the Fe K $\alpha$  emission-line flux cannot be trivially calculated from the EW. In some situations, it may be more appropriate, or easier, to compare and interpret the Fe K $\alpha$  line *flux* from different models (as opposed to the EW). In the present paper we calculate the *efficiency* of production of the Fe K $\alpha$  line, expressed as the ratio of the number of photons in the emission line to the number of photons in the illuminating continuum, above the Fe K edge absorption threshold energy. We utilize Monte Carlo results from the toroidal X-ray reprocessor model of Murphy & Yaqoob, described in detail in MY09, but we also discuss the generalization of our results to other geometries.

The paper is organized as follows. In §2 we give an overview of the details of the Monte Carlo model. In §3 we present the results for calculations of the efficiency of production of the Fe K $\alpha$  line in the context of a toroidal X-ray reprocessor model. In §4 we discuss the generalization of our results for other geometries and arbitrary covering factors. In §5 we apply our results to the well-known Seyfert galaxy MCG -6-30-15. We summarize our results and conclusions in §6.

## 2 TOROIDAL X-RAY REPROCESSOR MODEL

We have constructed a Monte-Carlo code to calculate grids of Green's functions to model the passage of X-rays through a toroidal reprocessor. The model, and some basic results, have been described in detail in MY09. Here we give a brief overview of the critical assumptions that the model is based upon. Our geometry is an azimuthally-symmetric doughnut-like torus with a circular cross-section, characterized by only two parameters, namely the half-opening angle,  $\theta_0$ , and the equatorial column density,  $N_H$  (see MY09 for details). The inclination angle between the observer's line of sight and the symmetry axis of the torus is given by  $\theta_{\text{obs}}$ , where  $\theta_{\text{obs}} = 0^\circ$  corresponds to a face-on observing angle and  $\theta_{\text{obs}} = 90^\circ$  corresponds to an edge-on observing angle (see MY09 for exact definitions of the face-on and edge-on angle bins). We assume that the X-ray source emits isotropically and that the reprocessing material is uniform and essentially neutral (cold). For illumination by an X-ray source that is emitting isotropically, the mean column density, integrated over all incident angles of rays through the torus, is  $\bar{N}_H = (\pi/4)N_H$ . The column density may also be expressed in terms of the Thomson depth:  $\tau_T = (11/9)N_H\sigma_T \sim 0.81N_{24}$  where  $N_{24}$  is the column density in units of  $10^{24} \text{ cm}^{-2}$ . Here, we have employed the mean number of electrons per H atom,  $\frac{1}{2}(1 +$

$\mu)$ , where  $\mu$  is the mean molecular weight. Note that this assumes that the abundance of He is 10% by number and that the number of electrons from all other elements aside from H and He is negligible (i.e.  $\mu = 13/9$ ).

The value of  $\theta_0$  for which we have calculated a comprehensive set of Green's functions is  $60^\circ$ , for  $N_H$  in the range  $10^{22-25} \text{ cm}^{-2}$ , using input energies up to 500 keV—see MY09 for details. For  $\theta_0 = 60^\circ$ , the solid angle subtended by the torus at the X-ray source,  $\Delta\Omega$ , is  $2\pi$  (and we refer to  $[\Delta\Omega/(4\pi)]$  as a covering factor, which in this case is 0.5). Our model employs a full relativistic treatment of Compton scattering, using the full differential and total Klein-Nishina Compton-scattering cross-sections. We utilized photoelectric absorption cross-sections for 30 elements as described in Verner & Yakovlev (1995) and Verner et al. (1996). We used Anders and Grevesse (1989) elemental cosmic abundances in our calculations. For the Fe K $\alpha$  and Fe K $\beta$  fluorescent emission lines, we used rest-frame line energies of 6.400 and 7.058 keV respectively, appropriate for neutral matter (e.g. see Palmeri et al. 2003). We used a fluorescence yield for Fe of 0.347 (see Bambynek et al. 1972) and an Fe K $\beta$  to Fe K $\alpha$  branching ratio of 0.135 (representative of the range of experimental and theoretical values discussed in Palmeri et al. 2003, see also Kallman et al. 2004).

## 3 EFFICIENCY OF PRODUCTION OF THE Fe K $\alpha$ LINE

Observational measurements of the equivalent width (EW) and/or flux of the fluorescent Fe K $\alpha$  emission line in the literature generally refer to the zeroth-order emission only, since the line is typically fitted with a Gaussian. The scattered flux (i.e., the Compton shoulder) can carry up to  $\sim 40\%$  of the zeroth-order flux, depending on the geometry and column density of the matter (e.g. Matt 2002; MY09). However, the scattered part of the line, or Compton shoulder, is generally not fitted (usually because it is not detected), or, if it is fitted, a separate EW or flux is quoted. On the other hand, part of the Compton shoulder may be blended with the zeroth-order line since most of the flux of the Compton shoulder spans an energy range that stretches from the zeroth-order line energy to  $\sim 6.25$  keV. The amount of blending depends on the column density, geometry, and orientation of the line emitter, as well as the velocity broadening and instrumental spectral resolution. However, in the remainder of the paper, the Fe K $\alpha$  line flux, intensity, luminosity, or EW, will always refer to the zeroth-order (unscattered) part of the emission line. Corrections for the Compton shoulder should be made that are appropriate for a particular situation.

We define the efficiency of production of the Fe K $\alpha$  emission line,  $x_{\text{Fe K}\alpha}$ , as the ratio of the line flux,  $I_{\text{Fe K}\alpha}$ , to the integrated flux in the incident X-ray continuum above the Fe K absorption edge threshold energy,  $E_K$ :

$$x_{\text{Fe K}\alpha} \equiv \frac{I_{\text{Fe K}\alpha}}{\int_{E_K}^{\infty} N(E) dE}. \quad (1)$$

Here,  $E_K$  is the threshold energy for Fe K-shell absorption, and we adopt the Verner et al. (1996) value of 7.124 keV. Assuming a power-law incident continuum, with photon index  $\Gamma$ ,

$$x_{\text{Fe K}\alpha} = \frac{I_{\text{Fe K}\alpha, n}}{\int_{E_K}^{\infty} E^{-\Gamma} dE} \quad (2)$$

$$= I_{\text{Fe K}\alpha, n} E_K^{\Gamma-1} (\Gamma - 1) \quad (\Gamma > 1), \quad (3)$$

where  $I_{\text{Fe K}\alpha, n}$  refers to the line flux renormalized to an incident continuum that has a monochromatic flux of 1 photon  $\text{cm}^{-2} \text{s}^{-1} \text{keV}^{-1}$  at 1 keV. The efficiency does not of course depend on the absolute normalization of the continuum. Note that the definition for the efficiency explicitly assumes that the intrinsic X-ray continuum emission is isotropic and emitted into a solid angle of  $4\pi$ . However,  $I_{\text{Fe K}\alpha, n}$  refers to the *observed* line flux so the efficiency may have an inclination-angle dependence. In the definition of  $x_{\text{Fe K}\alpha}$  we choose to use an upper limit of infinity because we find from our Monte Carlo simulations that when the medium becomes Compton-thick, downscattering of photons with initial energies much higher than even 20 keV to lower energies enables those high-energy photons to make significant contributions to the Fe K $\alpha$  line flux. This is illustrated in Fig. 1 which shows, for several column densities, the number of Fe K $\alpha$  emission-line photons resulting from continuum photons injected into the medium at an energy  $E$ , as a fraction of the number of line photons resulting from continuum photons injected at 7.2 keV (just above the Fe K absorption edge). For example, it can be seen that for  $N_H = 5 \times 10^{24} \text{ cm}^{-2}$  (dotted line, Fig. 1), the curve breaks at  $\sim 11$  keV, becoming flatter at higher energies. For  $N_H = 10^{25} \text{ cm}^{-2}$  (upper solid line, Fig. 1) the curve breaks and becomes flatter at  $\sim 15$  keV. An upper limit of infinity on the integral in equation 1 is also less arbitrary than choosing a specific value. In practice, the incident X-ray continuum in AGN will steepen and cut off at high energies (a few hundred keV in AGN – e.g. see Dadina 2008, and references therein). The effect of such a cut-off will give a somewhat larger efficiency than that given by equation 1. However, our purpose is to facilitate the estimation of the absolute Fe K $\alpha$  line flux; corrections required for different incident continua can easily be calculated. It is also worth mentioning that the absorption opacity above the Fe K edge is *not* due mostly to Fe. The ratio of the Fe K shell opacity to the sum of all of the other absorption opacities (for the cross-sections and abundances that we have adopted) is 0.51 just above the Fe K shell threshold energy, and never exceeds 0.61.

In the optically-thin limit for which absorption and scattering optical depths in the Fe K band ( $\sim 6\text{--}7$  keV) are  $\ll 1$ , we can obtain an analytic expression for  $x_{\text{Fe K}\alpha}$ . We can adopt the optically-thin expression for the Fe K $\alpha$  line EW in MY09 and multiply by the continuum at 6.4 keV in this limit. We get

$$x_{\text{Fe K}\alpha} = 0.00482 \left( \frac{\Delta\Omega}{4\pi} \right) \left( \frac{\omega_K}{0.347} \right) \left( \frac{\omega_{K\alpha}}{\omega_K} \right) \left( \frac{A_{\text{Fe}}}{4.68 \times 10^{-5}} \right) \\ \times \left( \frac{\sigma_0}{3.37 \times 10^{-20} \text{ cm}^2} \right) N_{22} f(\Gamma) \quad (\Gamma > 1), \quad (4)$$

where

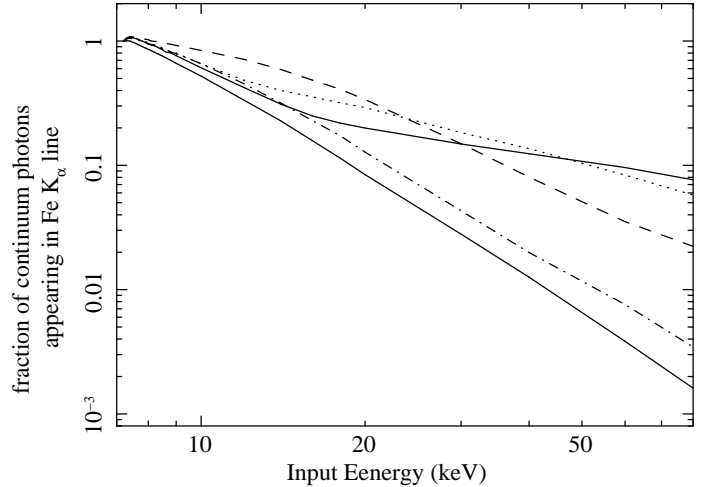


**Figure 1.** Monte Carlo results for the number of escaping Fe K $\alpha$  emission-line photons resulting from monoenergetic continuum photons injected into the toroidal X-ray reprocessor of Murphy & Yaqoob (2009) at an energy  $E$ , as a fraction of the number of line photons resulting from continuum photons injected at 7.2 keV. Results are shown for five equatorial column densities:  $2 \times 10^{23} \text{ cm}^{-2}$  (lower solid curve),  $5 \times 10^{23} \text{ cm}^{-2}$  (dot-dashed curve),  $2 \times 10^{24} \text{ cm}^{-2}$  (dashed curve),  $5 \times 10^{24} \text{ cm}^{-2}$  (dotted curve), and  $10^{25} \text{ cm}^{-2}$  (upper solid curve). For each column density, the Fe K $\alpha$  line photons that escape the medium are summed over all escape directions. As the reprocessor becomes more and more Compton-thick, the relative contribution to the Fe K $\alpha$  line from high-energy continuum photons increases significantly.

$$f(\Gamma) \equiv \frac{\Gamma - 1}{\Gamma + \alpha - 1} \quad (5)$$

The quantity  $[\Delta\Omega/(4\pi)]$  is the fractional solid angle that the line-emitting matter subtends at the X-ray source (and we refer to it synonymously as the covering factor). For the MY09 torus model,  $N_{22} = \bar{N}_H/(10^{22} \text{ cm}^{-2})$ , where  $\bar{N}_H = (\pi/4)N_H$  (see §2). The K-shell fluorescence yield is given by  $\omega_K$ , and  $\omega_{K\alpha}$  is the yield for the Fe K $\alpha$  line only (i.e. not including Fe K $\beta$ ). Using our adopted value of 0.135 for the Fe K $\beta$ /Fe K $\alpha$  branching ratio,  $\omega_{K\alpha}/\omega_K = 0.881$ . The quantity  $A_{\text{Fe}}$  is the Fe abundance relative to Hydrogen ( $4.68 \times 10^{-5}$  is the cosmic value in Anders & Grevesse 1989). The quantity  $\sigma_0$  is the Fe K shell absorption cross-section at the Fe K edge energy,  $E_K$ , and  $\alpha$  is the power-law index of the cross-section as a function of energy. For the Verner et al. (1996) data that we have adopted,  $\sigma_0 = 3.37 \times 10^{-20} \text{ cm}^2$ ,  $\alpha = 2.67$  (see MY09).

Using the MY09 toroidal X-ray reprocessor Monte Carlo results for  $[\Delta\Omega/(4\pi)] = 0.5$  and an input power-law continuum with  $\Gamma = 1.9$ , we constructed curves of the Fe K $\alpha$  line efficiency,  $x_{\text{Fe K}\alpha}$ , versus  $N_H$  using equation 1. Fig. 2 shows two such curves (solid lines), the upper and lower curves corresponding to the face-on and edge-on inclination-angle bins respectively. It can be seen that both curves show similar behavior. As  $N_H$  is increased,  $x_{\text{Fe K}\alpha}$  first increases but then turns over, reaching a maximum for  $N_H$  somewhere between  $\sim 3 - 8 \times 10^{23} \text{ cm}^{-2}$ , depending on the inclination angle. This is because the escape of Fe K $\alpha$  line photons from the medium after they are created is significantly impeded for larger column densities by absorption and scat-

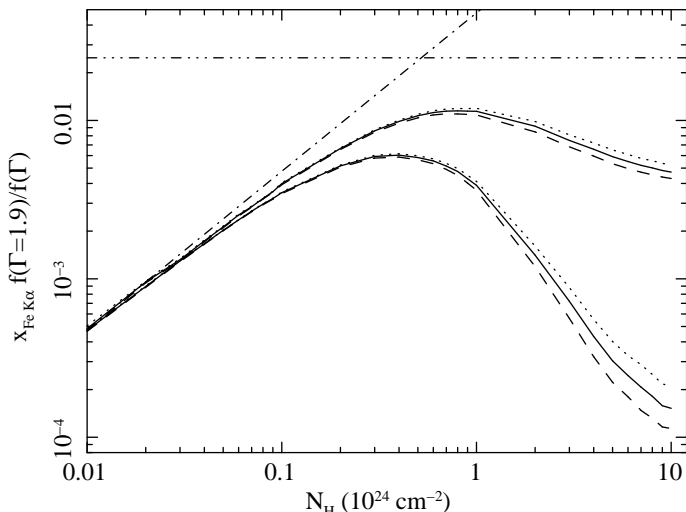


**Figure 2.** The Fe  $K\alpha$  line efficiency,  $x_{\text{Fe } K\alpha}$ , (defined in equation 1—see text) versus equatorial column density,  $N_{\text{H}}$ , for a toroidal X-ray reprocessor model with  $[\Delta\Omega/(4\pi)] = 0.5$ . When comparing with other geometries, the mean column density,  $(\pi/4)N_{\text{H}}$ , should be used. Solid curves correspond to a power-law incident continuum with  $\Gamma = 1.9$ . Dotted curves are for the same geometry but for  $\Gamma = 1.5$ , multiplied by the factor  $f(\Gamma = 1.9)/f(\Gamma = 1.5)$ , where  $f(\Gamma)$  is given by equation 5. Dashed curves correspond to  $\Gamma = 2.5$ , multiplied by the factor  $f(\Gamma = 1.9)/f(\Gamma = 2.5)$ . For each pair of curves for a given value of  $\Gamma$ , the upper and lower curves correspond to the face-on and edge-on inclination-angle bins respectively. The dot-dashed line shows the relation for the optically-thin limit (for  $\Gamma = 1.9$ ), from equation 4. The dashed, triple-dotted (horizontal) line shows the value of  $x_{\text{Fe } K\alpha}$  for a standard, face-on, semi-infinite disk that has a Compton-depth  $> 10$  ( $N_{\text{H}} > 1.25 \times 10^{25} \text{ cm}^{-2}$ ).

tering opacity that is relevant at the line energy. For the edge-on angle bin the maximum Fe  $K\alpha$  line efficiency is attained *well before the medium becomes Compton-thick* (i.e. before  $N_{\text{H}}$  becomes as high as  $1.25 \times 10^{24} \text{ cm}^{-2}$ ). This is also true of the angle-averaged maximum, which we find occurs at  $N_{\text{H}} \sim 4 \times 10^{23} \text{ cm}^{-2}$ . The position of the turnover can be understood as approximately corresponding to a situation for which the average optical depth to absorption plus scattering for the zeroth-order Fe  $K\alpha$  line photons is of order unity. The single-scattering albedo (ratio of scattering to total cross-section) at 6.4 keV, for the element abundances that we have adopted, is  $\sim 0.31$ . The optical depth to scattering is  $\sim 0.81\bar{N}_{\text{H}}/(10^{24} \text{ cm}^{-2})$ , or  $\sim 0.81(\pi/4)N_{24}$ , so putting  $0.81(\pi/4)N_{24}/0.31 \sim 1$  gives  $N_{24} \sim 0.5$  for the peak value of  $x_{\text{Fe } K\alpha}$ , agreeing well with our Monte Carlo results. For the covering factor of 0.5, it can be seen that the Fe  $K\alpha$  line efficiency is never more than  $\sim 1.15\%$ .

Also shown in Fig. 2 (dot-dashed line) is the optically-thin limit from equation 4. It can be seen that the Monte Carlo curves converge to this optically-thin limit, but only for column densities  $< 2 \times 10^{22} \text{ cm}^{-2}$ . It can also be seen that even for column densities as low as  $10^{23} \text{ cm}^{-2}$  (when the Thomson depth is only 0.08), errors as large as  $\sim 40\%$  can be incurred if one uses the optically-thin limit to calculate Fe  $K\alpha$  line fluxes and luminosities. This is because the important quantity that determines the observed fraction of Fe  $K\alpha$  line photons is the *total* opacity due to photo-

electric absorption and scattering. At 6.4 keV, the ratio of the absorption to scattering cross-section is  $\sim 7 : 3$  in our model. *Our results show that the optically-thin approximation should never be used to calculate or estimate Fe  $K\alpha$  line fluxes for  $N_{\text{H}} > 4 \times 10^{22} \text{ cm}^{-2}$  or so.* The error incurred in neglecting the opacity for Fe  $K\alpha$  line photons to escape the medium exceeds an order of magnitude (a factor of  $\sim 11$ ) for a column density of  $2 \times 10^{24} \text{ cm}^{-2}$  for the face-on bin, and is nearly two orders of magnitude for the edge-on bin (a factor of  $\sim 71$ ).

Although it is well-known that flatter incident continua give large Fe  $K\alpha$  line EWs and fluxes (e.g. MY09 and references therein), *the Fe  $K\alpha$  line efficiency is smaller for flatter incident continua* (lower values of  $\Gamma$ ). The reason is that steeper continua give a greater relative weight to the Fe K-shell absorption cross-section where it is largest (i.e. at lower energies down to the Fe K edge threshold energy). This can be seen clearly in equation 4 for the optically-thin limit, but it is true in general. We have calculated  $x_{\text{Fe } K\alpha}$  using various values of  $\Gamma$  from the MY09 toroidal X-ray reprocessor Monte Carlo results and find, rather surprisingly, that the  $x_{\text{Fe } K\alpha}$  versus  $N_{\text{H}}$  curves for different power-law slopes can be accounted for by the optically-thin factor,  $f(\Gamma)$  in equation 5, even up to column densities of  $\sim 2 \times 10^{24} \text{ cm}^{-2}$ . In other words if we have curves of  $x_{\text{Fe } K\alpha}$  versus  $N_{\text{H}}$  for  $\Gamma = 1.9$ , we can estimate the relation for a different value of  $\Gamma$  by multiplying the  $x_{\text{Fe } K\alpha}$  versus  $N_{\text{H}}$  relation for  $\Gamma = 1.9$  by the factor  $f(\Gamma)/f(\Gamma = 1.9)$ . This is illustrated in Fig. 2, where we have applied the process in reverse to the Monte Carlo results for the torus for  $\Gamma = 1.5$  (dotted curves) and  $\Gamma = 2.5$  (dashed curves), for the face-on and edge-on angle bins. This range in  $\Gamma$  of 1.5–2.5 covers values of the X-ray power-law continuum slope that is observationally-relevant for AGN. That is, we multiplied the actual Monte Carlo results for  $\Gamma = 1.5$  and  $\Gamma = 2.5$  by the factor  $f(\Gamma = 1.9)/f(\Gamma = 1.5)$  and  $f(\Gamma = 1.9)/f(\Gamma = 2.5)$  respectively. In the case that the approximation were perfect, the dotted, dashed, and solid curves in Fig. 2 would be identical for a given orientation of the reprocessor. We see from Fig. 2 that the error incurred in using this approximation to estimate  $x_{\text{Fe } K\alpha}$  from the  $\Gamma = 1.9$  results is *in the worst case* only  $\sim 11\%$  for the face-on angle bin (i.e. for the largest column density of  $10^{25} \text{ cm}^{-2}$  and  $\Gamma = 2.5$ ). For the edge-on angle bin the approximation is good to  $\sim 18\%$  or better up to  $N_{\text{H}} \sim 2 \times 10^{24} \text{ cm}^{-2}$  but increases with  $N_{\text{H}}$  up to  $\sim 37\%$  for  $N_{\text{H}} \sim 10^{25} \text{ cm}^{-2}$  and  $\Gamma = 2.5$ . We note that  $f(\Gamma = 1.5)/f(\Gamma = 1.9) \sim 0.63$ , and  $f(\Gamma = 2.5)/f(\Gamma = 1.9) \sim 1.43$ , so the absolute Fe  $K\alpha$  line efficiencies have a factor  $\sim 2.3$  range for a given column density as  $\Gamma$  varies in the observationally relevant range of 1.5–2.5. In the remainder of the present paper we shall refer to values of  $x_{\text{Fe } K\alpha}$  for  $\Gamma = 1.9$ . Results corresponding to other values of  $\Gamma$  can then be estimated using the method described above.

For reference, Fig. 2 also shows (dashed, triple-dotted line) the efficiency of Fe  $K\alpha$  line production for the standard case of a face-on, centrally-illuminated semi-infinite, Compton-thick disk (e.g. George & Fabian 1991) that subtends the same solid angle at the X-ray source as our default torus model (i.e.  $2\pi$ ). We calculated  $x_{\text{Fe } K\alpha}$  for the case of the disk using the `href1` disk-reflection continuum model (see Dovčiak, M., Karas, & Yaqoob 2004) for a power-law incident continuum with  $\Gamma = 1.9$ , and an EW for the Fe  $K\alpha$

line of 143 eV (from George & Fabian 1991). The Fe K $\alpha$  line efficiency for the disk is  $\sim 2.5\%$ , and is a constant in Fig. 2 because it corresponds to a disk with a Compton depth  $> 10$  ( $N_H > 1.25 \times 10^{25} \text{ cm}^{-2}$ ). The reason why the disk has a higher value of  $x_{\text{Fe K}\alpha}$  than the maximum for the torus (obtained for face-on reflection), even though both subtend a solid angle of  $2\pi$  at the X-ray source, is due to geometrical effects that have been discussed in detail in MY09.

### 3.1 Effect of Fe abundance and mild ionization

A higher abundance of Fe,  $A_{\text{Fe}}$ , will increase  $x_{\text{Fe K}\alpha}$ . In the optically-thin limit the increase in  $x_{\text{Fe K}\alpha}$  will be in direct proportion to  $A_{\text{Fe}}$ . However, the total absorption opacity at 6.4 keV also increases. If  $A_{\text{Fe}}$  increases by a factor 10, the absorption opacity at 6.4 keV increases by a factor of 2.5 and the total opacity to absorption plus scattering increases by a factor 2.0. Therefore, as the column density increases, the value of  $x_{\text{Fe K}\alpha}$  as a function of  $N_H$  will reach a maximum for smaller values of  $N_H$  relative to the case for cosmic Fe abundance. The maximum value for  $x_{\text{Fe K}\alpha}$  must be much less than the optically-thin value for these values of  $N_H$  and  $A_{\text{Fe}}$  (equation 4). Therefore, even if we increase  $A_{\text{Fe}}$  by a factor of 10 relative to the cosmic value, the maximum Fe K $\alpha$  line efficiency will only increase by much less than a factor of 10. We performed some Monte Carlo calculations using the MY09 toroidal reprocessor model with the Fe abundance increased by a factor 10 relative to the cosmic value and found that the maximum Fe K $\alpha$  line efficiency increased by a factor of  $\sim 2.8$ , to  $\sim 3.2\%$ , attained for a face-on inclination angle, and  $N_H \sim 3-4 \times 10^{23} \text{ cm}^{-2}$ . For an edge-on inclination angle the maximum value of  $x_{\text{Fe K}\alpha}$  increased by a factor of  $\sim 3.3$  relative to the cosmic Fe abundance value, to  $\sim 2\%$ , for  $N_H \sim 1-2 \times 10^{23} \text{ cm}^{-2}$ .

The calculations in the present paper pertain specifically to neutral matter. Ionization states of Fe higher than Fe XVII are not relevant to our discussion because we are making predictions for the Fe K $\alpha$  line in AGN that peaks at 6.4 keV. Even ionization states of Fe XVII give an Fe K $\alpha$  line energy that is higher than observed ( $\sim 6.43 \text{ keV}$  – e.g. Palmeri et al. 2003; Mendoza et al. 2004), and ionization states of Fe XII or lower are likely to be more appropriate (e.g. see Yaqoob et al. 2007). Mild ionization will have the effect of increasing the Fe K $\alpha$  line efficiency due to the reduced absorption opacities impeding the escape of line photons. We have investigated the effect of mild ionization on the Fe K $\alpha$  line efficiency in the context of the MY09 toroidal reprocessor model using a simple approach that gives a conservative upper limit on the Fe K $\alpha$  line efficiency. We used the XSTAR photoionization code (e.g. Kallman et al. 2004) to estimate the ionization parameter,  $\xi^*$ , for which the Fe K edge energy moves to  $\sim 7.4 \text{ keV}$  (appropriate for Fe XII – see Verner et al. 1996), up from the neutral Fe value of  $\sim 7.1 \text{ keV}$ . Although the geometry assumed by XSTAR is a spherical shell, our simple approach will still give a useful upper limit because in practice only the inner surface of the toroidal

reprocessor will be ionized but we simply substituted the total absorption opacities for all elements throughout the torus with the reduced opacities calculated by XSTAR. We used a column density of  $5 \times 10^{23} \text{ cm}^{-2}$  but calculated the absorption cross-sections per unit column density so that we could scale the cross-section for other column densities when applied in the toroidal Monte Carlo code. For a column density of  $5 \times 10^{23} \text{ cm}^{-2}$  we found an upper limit on  $\log \xi$  of 1.8 for the Fe K edge threshold energy to remain below  $\sim 7.4 \text{ keV}$ . Thus we used the total absorption cross-section for  $\log \xi = 1.8$  throughout the torus. Again, this procedure will underestimate the absorption at the energy of the Fe K $\alpha$  line, consistent with the goal of obtaining a conservative upper limit to the Fe K $\alpha$  line efficiency. We retained the K-shell cross-section for neutral Fe because it decreases slowly with increasing ionization state. We also retained the fluorescence yield for neutral Fe, which increases slowly with increasing ionization state. The changes in both K-shell cross-section and fluorescence yield are less than 15% up to Fe XVII, and the opposite sense of the changes tend to compensate each other (e.g. Bambynek et al. 1972) to some extent. We obtained the result that, using these very conservative assumptions, the maximum Fe K $\alpha$  line efficiency increases to 1.8%, the maximum being obtained for the same column density and orientation as the strictly neutral torus (i.e. a face-on inclination angle and  $N_H \sim 7-8 \times 10^{23} \text{ cm}^{-2}$ , or  $\bar{N}_H \sim 5.5-6.2 \times 10^{23} \text{ cm}^{-2}$ ). This corresponds to a maximum enhancement in the Fe K $\alpha$  line efficiency of  $\sim 50\%$  for mild ionization compared to the case of purely neutral matter.

## 4 OTHER GEOMETRIES AND COVERING FACTORS

In the limit when a medium is optically-thin to absorption and scattering in the Fe K band ( $\sim 6-7 \text{ keV}$ ), the relation between the Fe K $\alpha$  line efficiency and  $N_H$  is identical for all geometries for a given covering factor. The efficiency,  $x_{\text{Fe K}\alpha}$ , can then be found from equation 4 for any covering factor. The column density that is relevant for a given geometry is the average over all incident rays from the X-ray source, over all lines-of-sight that intercept the reprocessing structure. In terms of achieving the highest Fe K $\alpha$  line efficiency, there is a trade-off with the solid angle subtended by the structure at the X-ray source, or covering factor. Larger solid angles obviously intercept more continuum photons to produce more Fe K $\alpha$  line photons, but if the solid angle becomes too large, the escape of Fe K $\alpha$  line photons could be impeded (e.g. see discussion in Ikeda et al. 2009). The optimum opening angle for the maximum Fe K $\alpha$  line efficiency depends on the geometry and the observer's line-of-sight to the reprocessor. The maximum Fe K $\alpha$  line efficiency will always be achieved for lines of sight that are unobscured. For the toroidal geometry of MY09, a maximum efficiency,  $\sim 2.8\%$ , is achieved for a covering factor of  $[\Delta\Omega/(4\pi)] \sim 0.8-0.9$  for  $N_H \sim 8 \times 10^{23} \text{ cm}^{-2}$  (and a face-on orientation), before the medium becomes Compton-thick.

The MY09 Monte Carlo code is adaptable for different geometries and we have used it to compare the Fe K $\alpha$  line efficiency obtained from a toroidal geometry with the case of a centrally-illuminated, fully-covering sphere, and

\* Here we use the definition  $\xi \equiv L_{\text{ion}}/(nr^2)$ , where  $L_{\text{ion}}$  is the ionizing luminosity between 1–1000 Rydberg,  $n$  is the proton density, and  $r$  is the distance between the ionizing source and the illuminated surface of the matter.

an externally-illuminated sphere. For the former, we found that  $x_{\text{Fe K}\alpha}$  has a broad peak as a function of (radial)  $N_H$ , in the region  $\sim 3 - 5 \times 10^{23} \text{ cm}^{-2}$ , achieving a maximum value of  $\sim 1.6\%$ . In the case of the externally-illuminated sphere, we assumed a parallel beam incident on one side of the sphere and calculated  $x_{\text{Fe K}\alpha}$  as a function of the angle between the escaping line photons and the incident beam. In a clumpy medium the escaping line radiation would then consist of an appropriate angle-averaged spectrum over a distribution of such “blobs” (e.g. see also Nandra & George 1994; Miller, Turner, & Reeves, 2009 for discussion of such scenarios). The appropriate mean column density,  $\bar{N}_H$ , for an externally-illuminated sphere is 2/3 of the equatorial column density. We find that for an individual blob, not surprisingly, the maximum Fe K $\alpha$  line efficiency,  $\sim 2.6\%$ , is achieved for line photons escaping in a direction anti-parallel to the incident radiation, from the illuminated face, for  $\bar{N}_H \sim 8 \times 10^{23} \text{ cm}^{-2}$ . For this column density, the maximum efficiency for Fe K $\alpha$  line emission from the opposite face, parallel to the incident radiation is 2.1%, for  $\bar{N}_H \sim 6 - 7 \times 10^{23} \text{ cm}^{-2}$ . The angle-averaged value of  $x_{\text{Fe K}\alpha}$  (over  $0 - \pi$ ) peaks at 2.2% for  $\bar{N}_H \sim 5 - 6 \times 10^{23} \text{ cm}^{-2}$ . In addition to the angular averaging, for a clumpy medium one must account for the volume filling factor and covering factor of such blobs, and for interaction of line photons with multiple clouds. These effects can decrease the maximum Fe K $\alpha$  line efficiency, and in fact, as the covering factor and filling factor tend towards unity,  $x_{\text{Fe K}\alpha}$  has to tend to the value for a centrally-illuminated sphere, or  $\sim 1.6\%$ . For any reprocessor geometry, the general behavior of  $x_{\text{Fe K}\alpha}$  as a function of mean column density is the same. That is, a rise to a maximum, followed by a decline that is steeper the more heavily obscured the line of sight is. The column density for which the maximum is achieved will be in the range  $\sim 3 - 8 \times 10^{23} \text{ cm}^{-2}$ , with the largest values of  $\bar{N}_H$  and  $x_{\text{Fe K}\alpha}$  at the maximum corresponding to unobscured (pure reflection) lines of sight. However, none of the geometries that we have considered here (for cosmic abundances and neutral matter) give a value of  $x_{\text{Fe K}\alpha}$  greater than  $\sim 3\%$  (for  $\Gamma = 1.9$ ), for any covering factor, column density, or line of sight.

Our results also emphasize that the Fe K $\alpha$  emission line cannot be trivially used as a proxy for the intrinsic continuum luminosity in obscured AGN. It has been postulated that since the Fe K $\alpha$  line luminosity samples the intrinsic continuum over a large fraction of the sky, as seen from the X-ray source, it might be a good indicator of the intrinsic continuum luminosity, given that the line-of-sight may not be representative of the column density for the bulk of the reprocessor. However, we have shown that the dependence of the luminosity of the Fe K $\alpha$  line on the geometry, inclination angle,  $N_H$ , and  $A_{\text{Fe}}$  is sufficiently complex that such a use of the Fe K $\alpha$  line cannot be trivially implemented. In particular, as a function of  $N_H$ , the Fe K $\alpha$  line luminosity is double-valued. However, we can obtain a lower limit on the intrinsic luminosity. We have shown that regardless of geometry, inclination, and the column density of the reprocessor, for a given  $\Gamma$  and  $A_{\text{Fe}}$ , there is a maximum possible value for  $x_{\text{Fe K}\alpha}$  if one can be certain that the dominant species of Fe are Fe XII or less. We can measure  $\Gamma$ , and there may be independent constraints on  $A_{\text{Fe}}$ . Therefore, if we measure a flux or luminosity of the Fe K $\alpha$  line, the lower bound

on such a measurement implies a lower limit on the intrinsic continuum luminosity that corresponds to the maximum efficiency.

## 5 APPLICATION TO ABSORPTION-DOMINATED MODELS FOR MCG -6-30-15

We can apply our results to the case of the well-known Seyfert galaxy MCG -6-30-15. This AGN has been the archetypal X-ray source for harboring a broad, relativistic Fe K $\alpha$  line. However, Miller, Turner, & Reeves (2008) showed that absorption-dominated models that do not require a relativistically-broadened Fe K $\alpha$  line are also consistent with the X-ray data. Reynolds et al. (2009) claimed that such absorption-dominated models over-predict the flux of the narrow Fe K $\alpha$  emission-line at  $\sim 6.4 \text{ keV}$  and concluded that a finely-tuned model with a small covering factor is required. Here we show that this conclusion is invalid on the basis of simple physics.

MCG -6-30-15 has a typical narrow Fe K $\alpha$  line at 6.4 keV with a measured flux of  $1.6_{-0.9}^{+1.1} \times 10^{-5} \text{ photons cm}^{-2} \text{ s}^{-1}$  (Yaqoob & Padmanabhan 2004). The time-averaged 2–10 keV flux from a very long  $\sim 300 \text{ ks}$  *XMM-Newton* observation (Fabian et al. 2002; Dovčiak et al. 2004) was  $\sim 4.3 \times 10^{-11} \text{ erg cm}^{-2} \text{ s}^{-1}$  (a value this is representative of historical behavior—see Markowitz et al. 2003), and  $\Gamma = 1.9$  is typical. Therefore, we obtain a photon flux above the Fe K edge of  $2.8 \times 10^{-3} \text{ photons cm}^{-2} \text{ s}^{-1}$ . Using our general result of a maximum Fe K $\alpha$  line efficiency of  $\sim 3\%$  we get an Fe K $\alpha$  line flux of  $8.5 \times 10^{-5} \text{ photons cm}^{-2} \text{ s}^{-1}$ . Thus, no matter what distribution of cold/neutral matter that we place around the X-ray source in MCG -6-30-15, regardless of column density, covering factor, or geometry, we cannot obtain an Fe K $\alpha$  line flux much greater than  $8.5 \times 10^{-5} \text{ photons cm}^{-2} \text{ s}^{-1}$ . Miller et al. (2009) presented similar conclusions for the narrow Fe K $\alpha$  line flux in MCG -6-30-15. This is a very generous upper limit because it requires optimal values for the column density and covering factor, and a line-of-sight that does not intercept the line emitter. Obviously, a large column density in the line-of-sight will reduce the predicted Fe K $\alpha$  line flux. For example, for  $N_H = 2 \times 10^{24} \text{ cm}^{-2}$ , and a spherical geometry with a covering factor of 0.5, the predicted Fe K $\alpha$  line flux is very small, just  $\sim 4 \times 10^{-6} \text{ photons cm}^{-2} \text{ s}^{-1}$ . A similar value is obtained from the MY09 edge-on toroidal X-ray reprocessor model (see Fig. 2). Reynolds et al. (2009) obtained estimates of the Fe K $\alpha$  line flux in MCG -6-30-15 based on a simple cold, cosmic abundance absorber with  $N_H = 2 \times 10^{24} \text{ cm}^{-2}$ . However, they used an optically-thin approximation for a manifestly optically-thick scenario. Specifically, they used a column density that is one hundred times higher than the value for which that approximation begins to break down (see Fig. 2), and consequently obtained an effective efficiency that is unphysical. Reynolds et al. (2009) therefore obtained a very high Fe K $\alpha$  line flux ( $2.54 \times 10^{-4} \text{ photons cm}^{-2} \text{ s}^{-1}$ ) that is nearly two orders of magnitude higher than that expected for their assumed column density and covering factor ( $N_H = 2 \times 10^{24} \text{ cm}^{-2}$  and 0.35 respectively). They also gained a factor of  $\sim 2$  in the Fe K $\alpha$  line flux by assuming that *all* of the continuum photons absorbed above the Fe K

edge are absorbed by the Fe K shell, whereas in fact the true fraction is 0.51–0.61 (see §3).

## 6 SUMMARY

The Fe K $\alpha$  emission-line flux or luminosity is nontrivial to calculate because the optically-thin approximation (with respect to absorption and scattering in the  $\sim 6$ – $7$  keV band) breaks down for column densities as small as  $\sim 2 \times 10^{22}$  cm $^{-2}$ . Inappropriate use of the optically-thin approximation can lead to estimates of the line flux that are orders of magnitude too large. We have given a prescription for estimating the Fe K $\alpha$  line flux in the case of neutral matter with cosmic abundances, for some very general situations.

We have characterized the line flux in terms of a dimensionless *efficiency*,  $x_{\text{Fe K}\alpha}$ , defined as the ratio of the flux in the line to that in the incident continuum above the Fe K absorption edge threshold energy. We refer to values of  $x_{\text{Fe K}\alpha}$  that pertain to a power-law slope of the incident X-ray continuum of  $\Gamma = 1.9$  but have given a simple prescription for scaling  $x_{\text{Fe K}\alpha}$  to other values of  $\Gamma$  in the range 1.5–2.5. The maximum value of  $x_{\text{Fe K}\alpha}$  depends on the geometry, covering factor, and orientation, and is always obtained for lines of sight to the X-ray reprocessor that are unobscured. In general, this maximum is achieved before the structure becomes Compton-thick, for mean column densities in the range  $\sim 3 - 8 \times 10^{23}$  cm $^{-2}$ . For the toroidal geometry of MY09 the maximum Fe K $\alpha$  line efficiency is attained for nearly full covering ( $[\Delta\Omega/(4\pi)] \sim 0.9$ ), before the medium becomes Compton-thick, and is  $\sim 2.8\%$ . This can be compared with the maximum value of  $x_{\text{Fe K}\alpha}$  for a uniform, centrally-illuminated sphere of  $\sim 1.6\%$ . A clumpy distribution of matter can give somewhat higher Fe K $\alpha$  line efficiencies, of the order of 2%.

Regardless of geometry and covering factor, for cosmic abundances and incident continua with a power-law photon index of 1.9 or less, none of the geometries considered yields an Fe K $\alpha$  line efficiency greater than  $\sim 3\%$ . Steeper incident continua can give a higher efficiency but we find that for  $\Gamma = 2.5$  it is only a factor of  $\sim 1.43$  higher. X-ray sources that are Compton-thick in the line of sight can have Fe K $\alpha$  line efficiencies that are an order of magnitude or more smaller than the maximum for a given geometry. For example the MY09 toroidal geometry viewed edge-on has  $x_{\text{Fe K}\alpha} < 0.2\%$ , and  $x_{\text{Fe K}\alpha} < 0.02\%$  for column densities of  $2 \times 10^{24}$  cm $^{-2}$  and  $10^{25}$  cm $^{-2}$  respectively. We have applied our results to the Seyfert galaxy MCG  $-6$ -30-15 to show that absorption-dominated models for the broad, relativistic Fe K $\alpha$  emission line *do not* over-predict the flux of the narrow Fe K $\alpha$  line for any column density or covering factor. Recent claims to the contrary by Reynolds et al. (2009) are based on an invalid treatment of the problem. Our results also emphasize the fact that the absolute luminosity of the Fe K $\alpha$  emission line in obscured astrophysical sources cannot be used as a proxy for the intrinsic continuum luminosity in a trivial way. Using both the Fe K $\alpha$  line flux *and* EW does provide additional constraints but the intrinsic continuum luminosity may still be uncertain because of the complex dependencies upon Fe abundance, geometry, covering factor, and system orientation.

The authors thank Chris Done for carefully reviewing the manuscript and for helpful suggestions. Partial support from NASA grants NNG04GB78A (KM, TY) and NNX09AD01G (TY) is gratefully acknowledged. TJT acknowledges support from NASA grant NNX08AJ41G.

## REFERENCES

- Anders E., Grevesse N., 1989, *Geochimica et Cosmochimica Acta* 53, 197
- Bambynek W., Crasemann B., Fink R. W., Freund H.-U., Mark H., Swift C. D., Price R. E., Rao, P. V., 1972, *Rev. Mod. Phys.*, 44, 716
- Dadina M., 2008, *A&A*, 485, 417
- Dovčiak M., Karas V., Yaqoob T., 2004, *ApJS*, 153, 205
- Fabian A. C., Vaughan S., Nandra K. et al., 2002, *MNRAS*, 335, L1
- George I. M., Fabian A. C., 1991, *MNRAS*, 249, 352
- Ghisellini G., Haardt F., Matt, G., 1994, *MNRAS*, 267, 743
- Ikeda S., Awaki H., Terashima, Y., 2009, *ApJ*, 692, 608
- Kallman T. R., Palmeri P., Bautista M. A., Mendoza C., Krolik J. H., 2004, *ApJS*, 155, 675
- Krolik J. H., Madau P., Życki P. T., 1994, *ApJ*, 420, 57
- Leahy, D. A., & Creighton, J. 1993, *MNRAS*, 263, 314
- Levenson N. A., Heckman T. M., Krolik J. H., Weaver K. A., Życki P. T., 2006, *ApJ*, 648, 111
- Markowitz A., Edelson R., Vaughan S., 2003, *ApJ*, 598, 935
- Matt G., Pompilio F., La Franca F., 1999, *NewA*, 4, 191
- Matt G., 2002, *MNRAS*, 337, 147
- Mendoza C., Kallman T. R., Bautista M. A., Palmeri P., 2004, *A&A*, 414, 377
- Miller J., 2007, *ARA&A*, 45, 441
- Miller L., Turner T. J., Reeves J. N., 2008, *A&A*, 483, 437
- Miller L., Turner T. J., Reeves J. N., 2009, *MNRAS*, in press, astro-ph/0907.3114
- Murphy K. D., Yaqoob T., 2009, *MNRAS*, preprint, (astro-ph/0905.3188) (MY09)
- Nandra K., George I. M., 1994, *MNRAS*, 267, 974
- Palmeri P., Mendoza C., Kallman T. R., Bautista M. A., Melendez M. 2003, *A&A*, 410, 359
- Paul B., Dotani T., Nagase F., Mukherjee U., Naik S., 2005, *ApJ*, 627, 156
- Reynolds C. S., Fabian A. C., Brenneman L. W., Miniutti G., Uttley P., Gallo L. C., 2009, *MNRAS*, preprint, (astro-ph/0904.3099)
- Sulentic J. W., Marziani P., Zwitter T., Calvani M., Dultzin-Hacyan D., 1998, *ApJ*, 501, 54
- Verner D. A., Ferland G. J., Korista K. T., Yakovlev D. G., 1996, *ApJ*, 465, 487
- Verner D. A., Yakovlev D. G., 1995 *A&AS*, 109, 125
- Watanabe S., Sako M., Ishida M. et al., 2003, *ApJ*, 597, 37
- White N. E., Nagase F., Parmar A. N. 1995, in *X-ray Binaries*, ed. W. H. G. Lewin, J. van Paradijs (Cambridge: Cambridge University Press), p. 1
- Yaqoob T., Padmanabhan U., 2004, *ApJ*, 604, 63
- Yaqoob T., Murphy K. D., Griffiths R. D. et al., 2007, *PASJ*, 59S, 283